Journal of Medicinal Chemistry

Brief Article

pubs.acs.org/jmc

Exploring the Orthosteric Binding Site of the γ-Aminobutyric Acid Type A Receptor Using 4-(Piperidin-4-yl)-1-hydroxypyrazoles 3- or 5-Imidazolyl Substituted: Design, Synthesis, and Pharmacological Evaluation

Jacob Krall,[†] Claus H. Jensen,[†] Troels E. Sørensen,[†,§] Birgitte Nielsen,[†] Anders A. Jensen,[†] Tommy Sander,[‡] Thomas Balle,[§] and Bente Frølund*[,†]

[†]Department of Drug Design and Pharmacology, Faculty of Health and Medical Sciences, University of Copenhagen, Universitetsparken 2, DK-2100 Copenhagen, Denmark

[‡]Novo Nordisk A/S, Novo Allé, DK-2880 Bagsværd, Denmark

[§]Faculty of Pharmacy, The University of Sydney, Sydney, New South Wales, Australia

Supporting Information

ABSTRACT: A series of 4-(piperidin-4-yl)-1-hydroxypyrazole (4-PHP) 3- or 5-imidazolyl substituted analogues have been designed, synthesized, and characterized pharmacologically. All analogues showed binding affinities in the low micro- to low nanomolar range at native rat $GABA_A$ receptors and were found to be antagonists at the human $\alpha_1\beta_2\gamma_{2s}$ receptor. The structure−activity relationship of the compound series demonstrates distinct differences in size and architecture of previously discovered cavities in the vicinity of the 4-PHP scaffold in the orthosteric binding site.

INTRODUCTION

γ-Aminobutyric acid (GABA, Figure 1) is one of the major neurotransmitters in the mammalian central nervous system

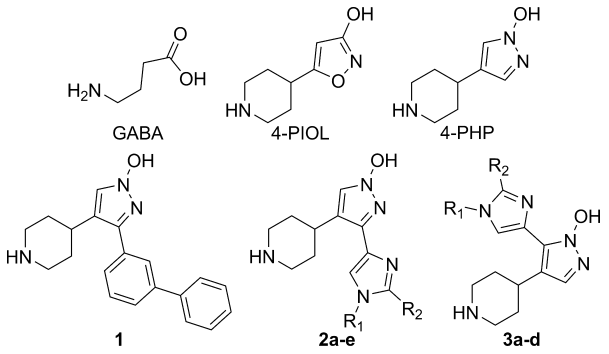

Figure 1. Structures of GABA, 4-PIOL, 4-PHP, **1**, and general structures of new 4-PHP analogues (**2a−e** and **3a−d**).

(CNS) and is responsible for the majority of the overall neuronal inhibition. The physiological effects of GABA are mediated through the ionotropic $GABA_A$ and the metabotropic $GABA_B$ receptors. The ionotropic $GABA_A$ receptors ($GABA_A$Rs) are widely distributed throughout the CNS where they play an essential role in numerous physiological processes. Furthermore, the $GABA_A$Rs have been linked to a variety of neurological and psychiatric disorders, e.g., Alzheimer's, Parkinson's, and Huntington's disease, epilepsy, anxiety, depression, schizophrenia, and cognitive disorders.[1]

The $GABA_A$Rs belong to the Cys-loop superfamily of pentameric ligand-gated ion-channels (LGICs) including the nicotinic acetylcholine receptors, the glycine receptors, the serotonin type 3 ($5\text{-}HT_3$) receptors, and a zinc-activated ion-channel.[2] The $GABA_A$Rs are transmembrane proteins assembled by five subunits to form a chloride-selective pentameric channel. To date, 19 different human $GABA_A$R subunits have been identified (α_{1-6}, β_{1-3},γ_{1-3}, δ, ε, π, θ, ρ_{1-3}). So far, the existence of 26 native $GABA_A$Rs have been proposed,[3,4] major combinations assembled being the $\alpha_1\beta_2\gamma_2$, $\alpha_3\beta_3\gamma_2$, and $\alpha_2\beta_3\gamma_2$ subtypes.[5] GABA binds at the interface of an α and a β subunit in the receptor complex.[6]

The three-dimensional structure of the $GABA_A$R is yet to be elucidated. Consequently, structure−activity relationship (SAR) studies and pharmacophore models have played a major role and are still essential in probing the structural basis for receptor−ligand interactions and the molecular determinants of ligand affinity, potency, efficacy, and subtype selectivity toward the $GABA_A$Rs. However, in recent years, valuable insight into the architecture of LGICs has been obtained. Several X-ray structures represent excellent templates for homology modeling of LGICs, including the $GABA_A$Rs. These templates comprises acetylcholine-binding proteins from various snails,[7−9] distantly related bacterial ion-channels,[10,11] and a recently published glutamate gated ion-channel.[12]

On the basis of multiple templates, we have previously presented homology models of the extracellular domain of the $GABA_A$R reflecting both the agonist- and antagonist-bound receptors.[13,14] Extensive SAR data, made available using the low efficacy partial agonists 5-(piperidin-4-yl)-3-isoxazolol (4-PIOL)[15−17] and 4-(piperidin-4-yl)-1-hydroxypyrazole (4-

Received: May 1, 2013

   dx.doi.org/10.1021/jm4006466 | J. Med. Chem. XXXX, XXX, XXX−XXX

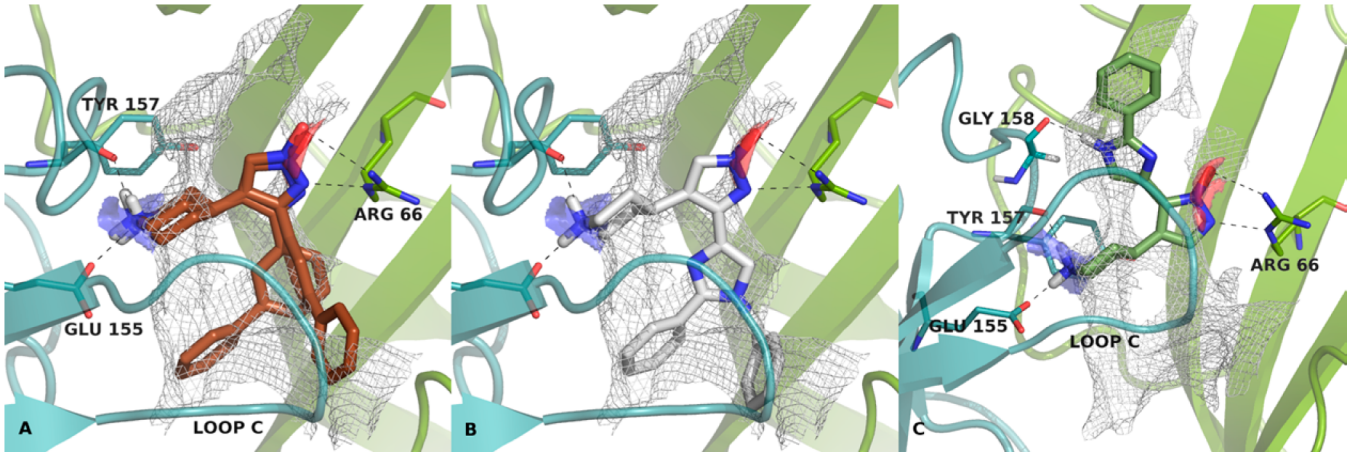

Figure 2. 4-PHP analogues **1** (A, brown), **2d** (B, white), and **3c** (C, green), respectively, docked into a homology model of the $\alpha_1\beta_2\gamma_2$ $GABA_AR$. Contours of favorable van der Waals interactions calculated with the program GRID are depicted with gray mesh (C3 probe, isolevel = −2 kcal/mol). Contours of favorable hydrogen bond acceptor sites are depicted with red surfaces (COO− probe, isolevel = −10 kcal/mol). Contours of favorable hydrogen bond donor sites are depicted with blue surfaces (N2+ probe, isolevel = −10 kcal/mol).

PHP) as scaffolds for a series of potent antagonists, including compound **1** (Figure 1),[18] has been part of the development of the above-mentioned models. On the basis of these studies, cavities near the 3- and the 5-position of the 4-PHP scaffold in the orthosteric binding site were identified.[14] The spaciousness of the cavities along with the ambiguity of binding modes led us to further challenge their boundaries with a series of imidazole substituted 4-PHP analogues (**2a−e** and **3a−d**, Figure 1). Here we report the design, synthesis, and pharmacological characterization of the compounds at native and recombinant $GABA_ARs$ and discuss the findings in the context of a homology model.

RESULTS AND DISCUSSION

Computational Modeling. Docking of compound **1** into the homology model[14] revealed two possible orientations with the 3-biphenyl substituent, either pointing "left" or "right", as illustrated in Figure 2A. In both orientations, GLIDE XP docking scores[19−22] are highly favorable, −10.6 ("left") and −9.8 ("right") kcal/mol, and in both orientations the core 4-PHP scaffold is placed with charged moieties within areas predicted by GRID[23,24] calculations to be favorable for a positively charged amine and a negatively charged carboxylic acid, respectively. GRID calculations of the binding site using a methyl probe (−2 kcal/mol), revealed a cavity below the 4-PHP scaffold toward the membrane region, denoted the "lower cavity". The more favorable docking score along with a better fit of the 3-biphenyl moiety within the favorable van der Waals contact area of the lower cavity suggests the "left" orientation to be the most likely binding mode in agreement with previous results.[14] Nonetheless, the alternative binding mode suggests ample space in the receptor to accommodate substituents even larger than the 3-biphenyl substituent in **1**. This led to the design of the imidazole analogue **2d**, which, as illustrated in Figure 3, addresses both predicted orientations simultaneously and when docked into the model (Figure 2B) the 1-benzyl-2-phenyl-4-imidazolyl substituent of **2d** overlaps almost perfectly with the unified binding modes for **1**.

The GRID calculations using the methyl probe also revealed a cavity above the 4-PHP scaffold away from the membrane region denoted the "upper cavity". The upper cavity is narrower, and docking studies suggests that it is capable of accommodating the 5-substituted 4-PHP analogue **3c** with a near perfect fit and furthermore predicts a hydrogen bond from the imidazole moiety to β_2-Gly158 (Figure 2C). However, unlike the lower cavity, the 4-PHP scaffolds bigger substituents are not predicted to contribute to increased affinity.

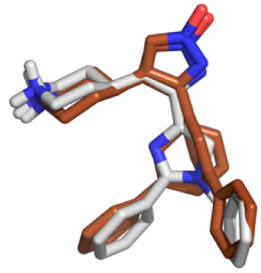

Figure 3. Overlay of **2d** (white) with both possible poses of **1** (brown).

A complete list of docking scores is listed in Supporting Information (SI).

Chemistry. Compounds **2a−e** and **3a−d** were all synthesized using the imidazole building blocks **4a−d** (please refer to SI for synthetic details) and core scaffolds **10** and **11** (Scheme 1), which were prepared as described previously.[18] Metal−halogen exchange of **4a,b,d** using ^{i}PrMgCl or direct deprotonation of the 4(5)-position of compound **4c** followed by quenching with tributyltin chloride formed the Stille reagent intermediates (not shown). These were used without purification in a Stille cross-coupling reaction using **10** *or* **11**, tetrakis(triphenylphosphine)Pd(0), copper(I) iodide, and cesium fluoride in DMF to form **12a−d** and **13a−d**. Acidic deprotection of **12a−d** and **13a−d** resulted in **2a−d** and **3a−d**, while compound **2e** was synthesized from **12b** by catalytic hydrogenation using 10% palladium on carbon followed by acidic deprotection.

Pharmacology. The synthesized compounds were characterized pharmacologically in binding studies using rat brain membrane preparations, where the binding affinities of **2a−e** and **3a−d** at native rat $GABA_ARs$ were measured by displacement of [^{3}H]muscimol. Functional characterization of **2a−e** and **3a−d** at the human ρ_1 (data not shown) and $\alpha_1\beta_2\gamma_{2S}$ $GABA_ARs$ transiently expressed in tsA201 cells was performed using the FLIPR Membrane Potential (FMP) Blue assay as

dx.doi.org/10.1021/jm4006466 | J. Med. Chem. XXXX, XXX, XXX−XXX

Scheme 1[a]

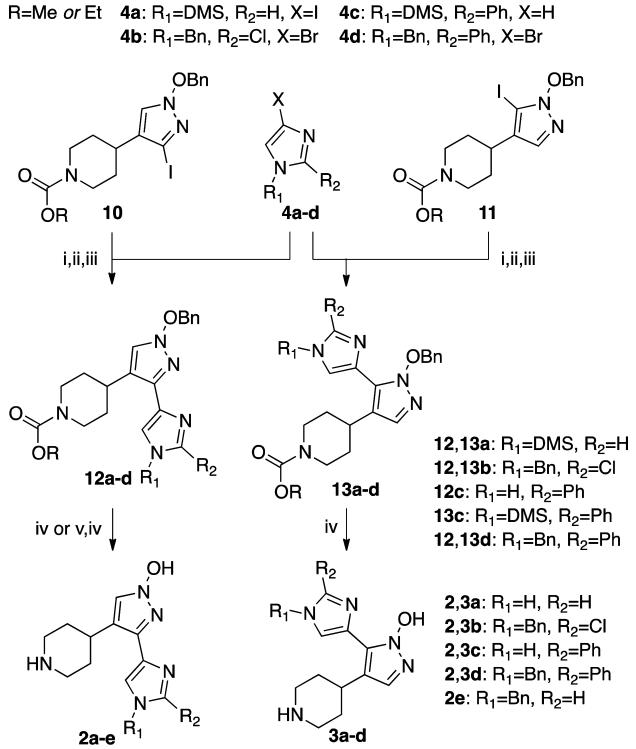

[a]Reagents and conditions: (i) **4a,b,d,** ^{i}PrMgCl, THF, rt, *or* **4c**, ^{n}BuLi, THF, −78 °C; (ii) Bu_3SnCl, THF, rt, *or* −78 °C to rt; (iii) **10** *or* **11**, $Pd(PPh_3)_4$, CuI, CsF, DMF, 45−110 °C; (iv) 48% aq. HBr, reflux; (v) 10% Pd/C, CH_2Cl_2, rt.

described previously[25] and in SI. The pharmacological characteristics of 4-PHP, **1**, **2a**−**e**, and **3a**−**d** in the radioligand binding and FMP assays are listed in Table 1.

The inhibitory potencies exhibited by the compounds in the FMP Blue assay are given as IC_{50} instead of K_i because of the mixed competitive/noncompetitive antagonistic profile we observed in the assay in a previous study.[26] The GABA concentrations used for the characterization of the antagonists in the assay were 2-fold higher than its EC_{50} at the $\alpha_1\beta_2\gamma_{2s}$ receptor. Thus, if the compounds were indeed completely competitive antagonists, as we expect them to be, the respective functional K_i for the compounds would be approximately 3 times lower than their IC_{50}.

Compounds **2a**,**c**,**d**, and **3c**,**d** were found to be antagonists with moderate to high potencies (0.21−30 μM) with **2d** showing antagonistic potency comparable to the standard $GABA_AR$ antagonist Gabazine.[15] The functional data are, in general, in good agreement with the binding affinity data. In contrast to the $\alpha_1\beta_2\gamma_{2s}$ data, none of the compounds displayed agonist or antagonist effects at the human ρ_1 $GABA_AR$ when tested at concentrations up to 300 μM.

Receptor Binding and Structure−Affinity Relationships. The 4-PHP analogues **2a**−**e** and **3a**−**d** all show binding affinities in the low micro- to low nanomolar range. The fact that **2a**−**e** and **3a**−**d** bind to the orthosteric binding site of the $GABA_ARs$ supports the presence of cavities capable of accommodating relatively large substituents, as previously suggested, in the vicinity of the 4-PHP scaffold in the orthosteric binding site.

The introduction of an unsubstituted imidazole in the 3- or 5-position of 4-PHP (**2a** and **3a**, respectively) does not affect

Table 1. Pharmacological Data for Gabazine, 4-PHP, 1, 2a−e, and 3a−d: $GABA_AR$ Binding Affinities at Rat Synaptic Membranes and Functional Characterization at the Human $\alpha_1\beta_2\gamma_{2S}$ $GABA_AR$ Transiently Expressed in tsA201 Cells in the FMP Blue Assay

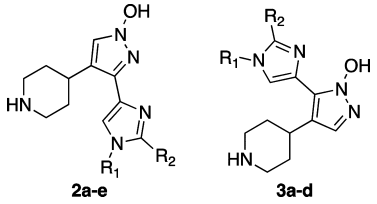

	R_1	R_2	[^{3}H]muscimol binding K_i (μM)[a] [pK_i ± SEM]	$\alpha_1\beta_2\gamma_{2S}$ tsA201 cell line IC_{50} (μM)[b] [pIC_{50} ± SEM]
Gabazine			0.074[c]	0.24[c]
4-PHP			10[d]	>500[d]
1			0.030[d]	0.21[d]
2a	H	H	5.1 [5.31 ± 0.08]	~30 [~4.5]
2b	Bn	Cl	0.74 [6.14 ± 0.02]	nd
2c	H	Ph	2.5 [5.61 ± 0.05]	9.7 [5.01 ± 0.06]
2d	Bn	Ph	0.28 [6.57 ± 0.05]	0.21 [6.67 ± 0.05]
2e	Bn	H	0.75 [6.13 ± 0.03]	nd
3a	H	H	7.5 [5.14 ± 0.08]	nd
3b	Bn	Cl	0.83 [6.09 ± 0.04]	nd
3c	H	Ph	0.014 [7.86 ± 0.04]	0.69 [6.16 ± 0.04]
3d	Bn	Ph	0.23 [6.64 ± 0.04]	0.78 [6.10 ± 0.08]

[a]IC_{50} values were calculated from inhibition curves and converted to K_i values. Data is given as the mean [mean pK_i ± SEM] of 3−4 independent experiments. [b]For the characterization of the antagonists, assay concentrations of GABA of 8 μM (EC_{85}−EC_{95}) were used. [c]From ref 15. [d]From ref 18. nd: not determined.

the binding affinity compared to 4-PHP substantially. Introduction of the larger 1-benzyl-2-chloro-4-imidazolyl substituent (**2b** and **3b**, respectively) and 1-benzyl-4-imidazolyl (**2e**) led to one order of magnitude enhancement in binding affinity compared to compound **2a** and **3a**, respectively. The identical binding affinity of **2b** and **2e** indicates that the chlorine in the 2-position of the 1-benzyl substituted imidazole has no influence on the binding affinity. Interestingly, introduction of a 2-phenyl-4-imidazolyl in **2a** (**2c**) did not affect the binding affinity compared to 4-PHP and **2a**, whereas a similar structural change in **3a** (**3c**) led to a 180-fold improvement in binding affinity compared to **3a**. This marked difference in binding affinity suggests that the introduced substituents in the 3- and 5-position of the 4-PHP scaffold project into different areas in the binding site. Docking studies (Figure 2C) suggest a possible interaction partner for the imidazole N−H hydrogen in **3c**, namely a hydrogen bond to β_2-Gly158. Furthermore, the more narrow upper cavity suggests a better complementarity of the substituent to the surrounding protein in the cavity compared to **2c** (please refer to SI for docking results of **2c**).

Combining the 1-benzyl and 2-phenyl imidazolyl substituents in compounds **2d** and **3d** leads to equivalent binding affinities for the two series of compounds. However, the introduction of the 1-benzyl group in **3d** led to a 16-fold loss in binding affinity compared to **3c**, whereas a similar introduction of a benzyl group in **2d** resulted in a 9-fold increase in binding affinity compared to **2c**. Again, the opposing effect in binding affinity for the two series of compounds, illustrated by **2d** and **3d**, supports our previous findings that the cavity above the 4-PHP

dx.doi.org/10.1021/jm4006466 | J. Med. Chem. XXXX, XXX, XXX−XXX

scaffold is more narrow than the cavity below, which has been shown to be able to accommodate more bulky substituents.[14]

The binding data and molecular modeling of **2d** (Figure 2B) indicate that the binding pocket is able to accommodate the disubstituted 1-benzyl-2-phenyl-4-imidazolyl introduced in the 3-position of 4-PHP, an area corresponding to the combined space occupied by the two possible orientations of the 3-biphenyl group of **1**. The similar high binding affinity shown for the corresponding analogue **3d** does not seem to fit with the homology model, where the limited space in the upper cavity of the binding site (Figure 2C) would hinder binding of the disubstituted 1-benzyl-2-phenyl-4-imidazolyl at the 5-position of 4-PHP. However, the SAR could be explained by the ligand turning 180° around the bond connecting the piperidine and 1-hydroxypyrazole moieties, thereby placing the bulky substituent in the more spacious lower cavity, which is also what is observed in docking studies (please refer to SI). This would not necessarily interfere with the salt-bridge formed between the 1-hydroxypyrazole moiety and α_1-Arg66 because the negative charge is distributed between the oxygen and the pyrazole N2.

CONCLUSION

On the basis of a previously reported homology model of the $\alpha_1\beta_2\gamma_2$ $GABA_AR$, a new series of 4-PHP 3- or 5-imidazolyl-substituted analogues (**2a−e** and **3a−d**) has been designed, synthesized, and characterized pharmacologically at $GABA_ARs$. All analogues showed low micro- to low nanomolar binding affinities. Ligand−receptor docking suggests a common binding mode for the core 4-PHP scaffold with the 3- (**2a−e**) and 5-substituents (**3a−c**), addressing two different cavities in the vicinity of the 4-PHP scaffold. The SAR data from the present study indicates that the area surrounding the 3-position of 4-PHP is more receptive to larger substituents than the cavity at the 5-position of 4-PHP. In turn, the equipotency of **2d** and **3d** may be explained by a 180° flip of **3d** to place the bulky substituent in the larger lower cavity. Altogether, these new results offer a more detailed insight into the architecture of the orthosteric binding site in the antagonist binding mode of $GABA_ARs$.

EXPERIMENTAL SECTION

Chemistry. The syntheses of selected compounds are described below as representative. The purity of all tested compounds was analyzed using combustion analysis or HPLC. Elementary analyses calculated are within 0.4% of found values, and HPLC purity is ≥95% unless otherwise stated.

General Procedure for Stille Cross-Coupling (12a−d, 13a−d). The imidazole **4a,b,d** (1 equiv) in CH_2Cl_2 or THF was added to ^{i}PrMgCl (1.2−2.3 equiv), while **4c** in THF at −78 °C was added to ^{n}BuLi (1.1 equiv). The solutions were stirred for 30 min before addition of Bu_3SnCl (1.1−1.4 equiv). The resulting mixtures were stirred overnight at rt before removal of solvent. The crude Stille reagent was dissolved in DMF and **10** or **11** (1 equiv), CuI (0.1−0.3 equiv), CsF (2.0 equiv), $Pd(PPh_3)_4$ (0.05 equiv) were added and flushed with N_2. The reaction was stirred for 45−110 °C for 3−8 days before standard workup. The crude product was purified using DCVC.

ASSOCIATED CONTENT

Supporting Information

Synthesis details, ^{1}H NMR and ^{13}C NMR of synthesized compounds, elementary analyses of all new target compounds, pharmacological methods, and molecular modeling methods. This material is available free of charge via the Internet at http://pubs.acs.org.

AUTHOR INFORMATION

Corresponding Author

*Phone: +45 35336495. Fax: +45 35336040. E-mail: bfr@sund.ku.dk.

Notes

The authors declare no competing financial interest.

ACKNOWLEDGMENTS

J.K. and T.E.S. were supported by The Danish Medical Research Council and A.A.J. was supported by the Novo Nordisk and Carlsberg Foundations.

ABBREVIATIONS USED

DCVC, dry column vacuum chromatography; FLIPR, fluorescent imaging plate reader; FMP, FLIPR membrane potential; GABA, γ-aminobutyric acid; $GABA_ARs$, γ-aminobutyric acid type A receptors; 5-HT, 5-hydroxytryptamine; 4-PIOL, 5-(piperidin-4-yl)-3-isoxazolol; 4-PHP, 4-(piperidin-4-yl)-1-hydroxypyrazole; SAR, structure−activity relationship

REFERENCES

(1) Foster, A. C.; Kemp, J. A. Glutamate- and GABA-based CNS therapeutics. *Curr. Opin. Pharmacol.* **2006**, *6*, 7−17.

(2) Thompson, A. J.; Lester, H. A.; Lummis, S. C. R. The structural basis of function in Cys-loop receptors. *Q. Rev. Biophys.* **2010**, *43*, 449−499.

(3) Sarto-Jackson, I.; Sieghart, W. Assembly of $GABA_A$ receptors (review). *Mol. Membr. Biol.* **2008**, *25*, 302−310.

(4) Olsen, R. W.; Sieghart, W. International Union of Pharmacology. LXX. Subtypes of γ-aminobutyric acid A receptors: classification on the basis of subunit composition, pharmacology, and function. Update. *Pharmacol. Rev.* **2008**, *60*, 243−260.

(5) Whiting, P. J. GABA-A receptor subtypes in the brain: a paradigm for CNS drug discovery? *Drug Discovery Today* **2003**, *8*, 445−450.

(6) Sieghart, W.; Sperk, G. Subunit composition, distribution and function of $GABA_A$ receptor subtypes. *Curr. Top. Med. Chem.* **2002**, *2*, 795−816.

(7) Brejc, K.; van Dijk, W. J.; Klaassen, R. V.; Schuurmans, M.; van der Oost, J.; Smit, A. B.; Sixma, T. K. Crystal structure of an ACh-binding protein reveals the ligand-binding domain of nicotinic receptors. *Nature* **2001**, *411*, 269−276.

(8) Celie, P. H. N.; van Rossum-Fikkert, S. E.; van Dijk, W. J.; Brejc, K.; Smit, A. B.; Sixma, T. K. Nicotine and carbamylcholine binding to nicotinic acetylcholine receptors as studied in AChBP crystal structures. *Neuron* **2004**, *41*, 907−914.

(9) Hansen, S. B.; Sulzenbacher, G.; Huxford, T.; Marchot, P.; Taylor, P.; Bourne, Y. Structures of *Aplysia* AChBP complexes with nicotinic agonists and antagonists reveal distinctive binding interfaces and conformations. *EMBO J.* **2005**, *24*, 3635−3646.

(10) Hilf, R. J. C.; Dutzler, R. X-ray structure of a prokaryotic pentameric ligand-gated ion channel. *Nature* **2008**, *452*, 375−379.

(11) Bocquet, N.; Nury, H.; Baaden, M.; Le Poupon, C.; Changeux, J.-P.; Delarue, M.; Corringer, P.-J. X-ray structure of a pentameric ligand-gated ion channel in an apparently open conformation. *Nature* **2009**, *457*, 111−114.

(12) Hibbs, R. E.; Gouaux, E. Principles of activation and permeation in an anion-selective Cys-loop receptor. *Nature* **2011**, *474*, 54−60.

(13) Bergmann, R.; Kongsbak, K.; Sørensen, P. L.; Sander, T.; Balle, T. A unified model of the $GABA_A$ receptor comprising agonist and benzodiazepine binding sites. *PLoS ONE* **2013**, *8*, e52323.

(14) Sander, T.; Frølund, B.; Bruun, A. T.; Ivanov, I.; McCammon, J. A.; Balle, T. New insights into the $GABA_A$ receptor structure and orthosteric ligand binding: receptor modeling guided by experimental data. *Proteins: Struct., Funct., Bioinf.* **2011**, *79*, 1458−1477.

(15) Frølund, B.; Jørgensen, A. T.; Tagmose, L.; Stensbøl, T. B.; Vestergaard, H. T.; Engblom, C.; Kristiansen, U.; Sanchez, C.;

Krogsgaard-Larsen, P.; Liljefors, T. Novel class of potent 4-arylalkyl substituted 3-isoxazolol $GABA_A$ antagonists: synthesis, pharmacology, and molecular modeling. *J. Med. Chem.* **2002**, *45*, 2454−2468.
(16) Frølund, B.; Jensen, L. S.; Guandalini, L.; Canillo, C.; Vestergaard, H. T.; Kristiansen, U.; Nielsen, B.; Stensbøl, T. B.; Madsen, C.; Krogsgaard-Larsen, P.; Liljefors, T. Potent 4-aryl- or 4-arylalkyl-substituted 3-isoxazolol $GABA_A$ antagonists: synthesis, pharmacology, and molecular modeling. *J. Med. Chem.* **2005**, *48*, 427−439.
(17) Frølund, B.; Jensen, L. S.; Storustovu, S. I.; Stensbøl, T. B.; Ebert, B.; Kehler, J.; Krogsgaard-Larsen, P.; Liljefors, T. 4-Aryl-5-(4-piperidyl)-3-isoxazolol $GABA_A$ antagonists: synthesis, pharmacology, and structure−activity relationships. *J. Med. Chem.* **2007**, *50*, 1988−1992.
(18) Møller, H. A.; Sander, T.; Kristensen, J. L.; Nielsen, B.; Krall, J.; Bergmann, M. L.; Christiansen, B.; Balle, T.; Jensen, A. A.; Frølund, B. Novel 4-(piperidin-4-yl)-1-hydroxypyrazoles as γ-aminobutyric $acid_A$ receptor ligands: synthesis, pharmacology, and structure−activity relationships. *J. Med. Chem.* **2010**, *53*, 3417−3421.
(19) *Glide*, version 5.8; Schrödinger, LLC:New York, 2012.
(20) Friesner, R. A.; Banks, J. L.; Murphy, R. B.; Halgren, T. A.; Klicic, J. J.; Mainz, D. T.; Repasky, M. P.; Knoll, E. H.; Shelley, M.; Perry, J. K.; Shaw, D. E.; Francis, P.; Shenkin, P. S. Glide: a new approach for rapid, accurate docking and scoring. 1. Method and assessment of docking accuracy. *J. Med. Chem.* **2004**, *47*, 1739−1749.
(21) Halgren, T. A.; Murphy, R. B.; Friesner, R. A.; Beard, H. S.; Frye, L. L.; Pollard, W. T.; Banks, J. L. Glide: a new approach for rapid, accurate docking and scoring. 2. Enrichment factors in database screening. *J. Med. Chem.* **2004**, *47*, 1750−1759.
(22) Friesner, R. A.; Murphy, R. B.; Repasky, M. P.; Frye, L. L.; Greenwood, J. R.; Halgren, T. A.; Sanschagrin, P. C.; Mainz, D. T. Extra Precision Glide: docking and scoring incorporating a model of hydrophobic enclosure for protein−ligand complexes. *J. Med. Chem.* **2006**, *49*, 6177−6196.
(23) Goodford, P. J. A computational procedure for determining energetically favorable binding sites on biologically important macromolecules. *J. Med. Chem.* **1985**, *28*, 849−857.
(24) *GRID*, version 22c; Molecular Discovery, Ltd: Pinner, Middlesex, UK, 2009.
(25) Jensen, A. A.; Bergmann, M. L.; Sander, T.; Balle, T. Ginkgolide X is a potent antagonist of anionic Cys-loop receptors with a unique selectivity profile at glycine receptors. *J. Biol. Chem.* **2010**, *285*, 10141−10153.
(26) Krehan, D.; í Storustovu, S.; Liljefors, T.; Ebert, B.; Nielsen, B.; Krogsgaard-Larsen, P.; Frølund, B. Potent 4-arylalkyl-substituted 3-isothiazolol $GABA_A$ competitive/noncompetitive antagonists: synthesis and pharmacology. *J. Med. Chem.* **2006**, *49*, 1388−1396.